2.B *Nuclear Physics* **86** (1966) 363—377; © *North-Holland Publishing Co., Amsterdam*

ELASTIC AND INELASTIC SCATTERING OF 15.8 MeV DEUTERONS

A. A. COWLEY, G. HEYMANN and R. L. KEIZER
Council for Scientific and Industrial Research, Pretoria, South Africa
and
MARY JEAN SCOTT
University of the Witwatersrand, Johannesburg, South Africa

Received 30 March 1966

Abstract: Absolute differential cross sections were measured for elastic and inelastic scattering of 15.8 MeV deuterons from ^{9}Be, ^{12}C, ^{16}O, ^{27}Al and ^{32}S. Measurements were taken at angular intervals (lab) of 2.5° ($5° < \theta < 60°$) and 5° ($60° < \theta < 155°$). The angular resolution varied from $\pm 0.1°$ to $\pm 1.0°$. Background was reduced using $E\Delta E$ coincidences to identify scattered deuterons. The elastic differential cross sections show a marked interference pattern at large angles; at small (c.m.) angles (9.5° for ^{9}Be and 13.0° for ^{32}S) the cross sections are purely Rutherford. The Blair model, the unified strong absorption model of Frahn and Venter and the optical model were used to analyse the elastic scattering cross sections.

E NUCLEAR REACTIONS Be, C, O, Al, S(d, d), (d, d'), E = 15.8 MeV; measured $\sigma(E_{d'}, \theta)$. Natural targets.

1. Introduction

The success of the strong absorption diffraction mechanism in explaining the elastic and inelastic scattering of alpha particles [1,2]) has stimulated a renewed interest in the mechanism of both elastic and inelastic deuteron scattering [3,4]). As the alpha particle is a tightly bound structure, while the deuteron is loosely bound, it is an open question whether strong absorption diffraction also plays an important role in the scattering of deuterons, particularly in the case of light nuclei. The present work was undertaken to study the applicability of a diffraction scattering analysis to 15.8 MeV deuteron scattering from ^{9}Be, ^{12}C, ^{16}O, ^{27}Al and ^{32}S. The experimental results are analysed in terms of two strong absorption diffraction scattering models. In a first attempt to determine whether a strong absorption model can be applied to the cases under consideration, a sharp cut-off model as developed by Blair and others [1]) was used. After establishing that the elastic scattering does show a diffraction pattern, the results were interpreted in terms of another strong absorption model in which the unit step function or sharp cut-off assumption is replaced by a smooth function. This smoothing function gives a more gradual transition, over the nuclear surface, from the opaque nuclear interior to the region of no absorption outside the nucleus. Such

a model, developed by Frahn and Venter [5]) for alpha-particle scattering, was used in the present case with the assumption of zero spin for the deuteron. The results of these four-parameter analyses are compared with those obtained from fitting our data with the optical model.

2. Experimental Procedure

The experimental arrangement is shown in fig. 1. The CSIR cyclotron accelerated deuterons to an energy of 15.8 MeV. Two quadrupole magnets focussed the beam and the steering magnet corrected small deviations of the beam from the centre of the scattering chamber.

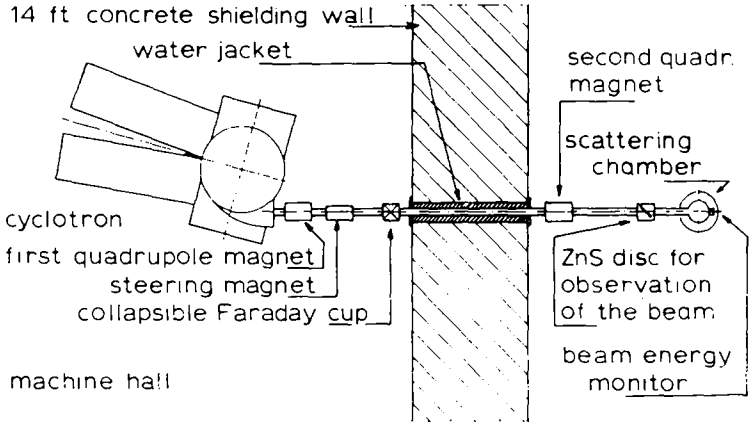

Fig. 1. Lay-out of the machine hall, experimental hall and scattering experiment.

The scattering chamber is shown in fig. 2. The apparatus consisted of a circular steel plate attached to a triangular frame. Scale marks were engraved on the circumference of the plate at intervals of 1°, covering 360°, to an accuracy better than 0.01°. A shaft was mounted in the centre of this plate and two arms could revolve around this shaft. One arm carried the $E\Delta E$ counter while the other arm supported the monitor counter. The central shaft supported the cylindrical scattering chamber which had an inside diameter of 304 mm and an inside height of 174 mm. The target holder was mounted on the removable top plate. An engraved scale on the top of the lid permitted the target angle to be set to an accuracy of better than 0.5°. The scattering chamber had two beam entrance ports A and B, in which the collimator assembly could be mounted. Port A was used for measurements in the angular range from 16° to 157°, while port B was used for measurements from 4° to 25°. For absolute cross section measurements the Faraday cup, with an acceptance angle of ±5° from the target, was used. Slits (19 mm high) were machined in the walls of the scattering chamber and covered with 25 μm Melinex foil, so that the reaction products from the target

could be detected outside the chamber. The collimator assembly consisted of four lead collimators, two of which were used to define the beam and the other two as anti-scattering baffles. The maximum error in the beam direction was 0.3°, the maximum divergence was $\pm 0.4°$; the diameters of the defining apertures were 5 mm. This yielded an aperture slightly larger than the area illuminated by the beam when focussed on the target with the collimators removed.

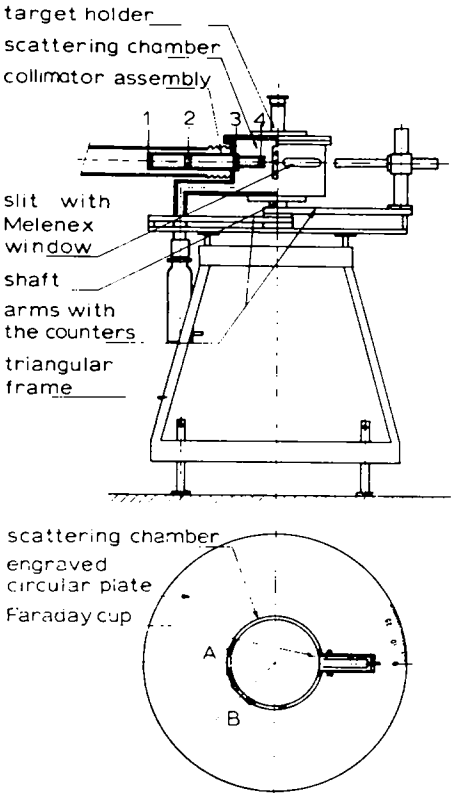

Fig. 2. Scattering chamber and support.

3. Electronics

Charged particle identification and background reduction were obtained by using an $E\Delta E$ coincidence method. The ΔE pulses were obtained from a 0.2 mm thick CsI(Tl) crystal with an energy resolution of 15 %. The energy resolution of the CsI (Tl) E-crystal, which stopped the deuterons, was 2.5 % for 15.8 MeV deuterons, using a Dumont 6292 phototube. The theory underlying this method has been widely described [6-8]).

4. Cross-Section Measurements

The ^{9}Be and ^{27}Al targets were made of commercially available foil, 4.5 mg/cm^2 and 2.2 mg/cm^2 thick, respectively. The ^{12}C targets were either polystyrene foil or were produced by painting a mixture of Aquadag and alcohol on clean glass plates. The targets were 2–4 mg/cm^2 thick. The ^{16}O targets used were either 2.5 mg/cm^2 Melinex foil or 0.4 mg/cm^2 Al_2O_3 foil prepared by the method of Hauser and Kerler [9]). The sulphur targets, 3–6 mg/cm^2 thick, were rolled from black plastic sulphur, which was produced by pouring hot liquid sulphur at a temperature exceeding 200 °C into cold water. The sulphur targets were not very resistant to the beam so that a large number were used in this experiment. All targets were of natural isotopic abundance.

The measurements were done at 2.5° intervals in the laboratory angular range from 5° to 60° and at 5.0° intervals in the range from 60° to 155°. Absolute cross sections were measured for ^{9}Be, ^{12}C, ^{16}O and ^{27}Al. For ^{32}S no absolute measurements could be done because the targets disintegrated rapidly under deuteron bombardment. Relative cross sections were therefore obtained by normalizing detector counts to monitor counts. In order to obtain the absolute cross section a normalization was done at small angles where the cross section was assumed to correspond to pure Rutherford scattering.

The cross-section measurements were reproducible within 10 %, while the estimated accuracy of the absolute cross section is 15 %. At angles smaller than 12°, the errors in the inelastic cross sections are of the order of 30 %, since high background subtractions were necessary. The mean angle of scattering in the interval from 5° to 25° was determined to about 1.0° by scattering to the right and left of the incident beam. At angles between 25° and 155° the error was estimated to be smaller than 1.0°. The energy of the deuteron beam was 15.8 ± 0.15 MeV. No corrections were made for target thickness.

The elastic cross sections as functions of scattering angle in the c.m. system for ^{9}Be, ^{12}C, ^{16}O, ^{27}Al and ^{32}S are shown in figs. 3–5. The numerical values of the elastic and inelastic cross sections are given in the appendix.

5. Discussion

5.1. GENERAL

The theories applied to the elastic scattering results were the sharp cut-off model as developed by Blair [1,4]), the unified strong absorption model (USAM) as developed by Frahn and Venter [5]) and the optical model. Considering the assumptions made, each of the three models is well established in its own field of applicability. However, for deuteron scattering in the low mass region under consideration, the limits of the assumptions in each model are approached. The fits obtained with the Blair model are as good as can be expected from this model, thereby establishing that the elastic

scattering can be represented in terms of a diffraction picture. This was the incentive to attempt fitting the data to the other two models.

5.2. THE BLAIR MODEL

If Coulomb effects are neglected and the sharp cut-off assumption is made, the cross section for elastic scattering of deuterons may be written as

$$d\sigma/d\Omega = (\cos^2 \tfrac{1}{2}\theta)(kR_0)^2[J_1(x)/x]^2, \tag{1}$$

where $x = 2kR_0 \sin \tfrac{1}{2}\theta$, k is the c.m. wave number of the incoming particle, θ the

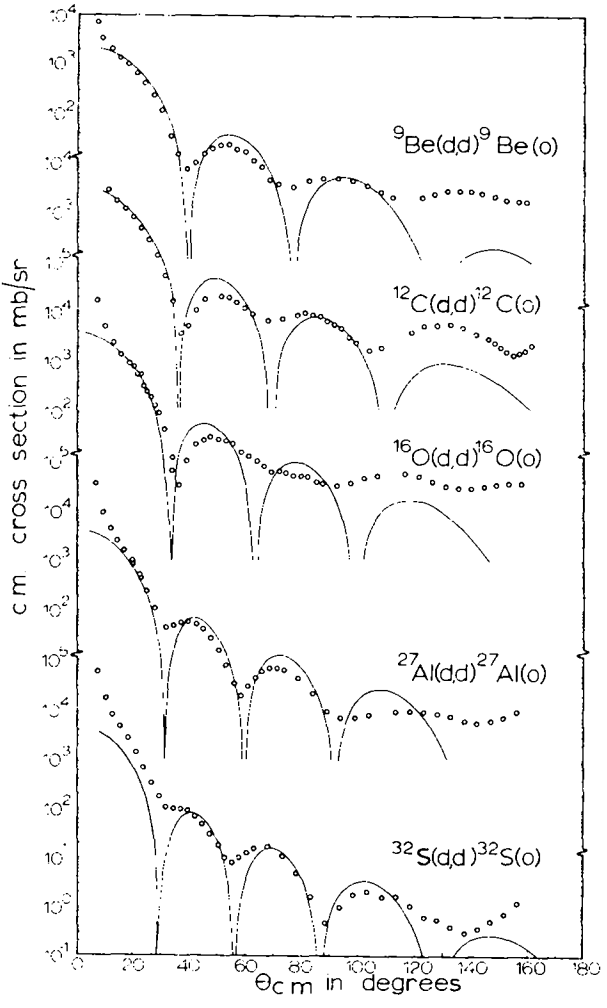

Fig. 3. The cross sections for elastic scattering of deuterons from ^{9}Be, ^{12}C, ^{16}O, ^{27}Al and ^{32}S as a function of scattering angle. The circles are the experimental points and the solid lines are the Blair-model fits.

c.m. scattering angle and R_0 the interaction radius for plane waves, which was calculated by considering the positions of the maxima and minima of the experimental cross-section curves. This formula is accurate only for small angle scattering because of approximations made in the derivation.

The extraction of the sharp cut-off radius R_0 is in effect the determination of the interaction radius for deuterons which move at large distances from the nucleus and are scattered through small angles. As is expected therefore, the elastic cross section is well predicted at forward angles. Qualitative agreement is obtained for the higher order maxima. The extracted interaction radii increase with mass number; however, the number of elements which has been presented is insufficient to draw any conclusions.

5.3. THE UNIFIED STRONG ABSORPTION MODEL

In USAM the sharp cut-off condition is replaced by the assumption that there is a gradual transition in the absorptive properties at the nuclear surface with respect to the partial waves taking part in the scattering. In a partial wave expansion the amplitude for elastic scattering of charged, spin zero, particles is given by

$$f(\theta) = f_C(\theta) - \frac{i}{2k}\sum_{l=0}^{\infty}(2l+1)[\eta_l \exp(-2i\sigma_l) - 1][\exp 2i\sigma_l]P_l(\cos\theta),$$

where $f_C(\theta)$ is the Coulomb amplitude and k the wave number of relative motion. The parameters η_l and σ_l are the amplitude and Coulomb phase shift, respectively, of the lth outgoing partial wave. The Legendre polynomial of order l is indicated by $P_l(\cos\theta)$. In the phenomenological approach of Frahn and Venter the absorptive properties of the transition zone are expressed in terms of a function $g(t)$ given by

$$\mathrm{Re}[\eta_l \exp(-2i\sigma_l)] = g(t), \tag{2}$$

and the refractive properties by

$$\mathrm{Im}[\eta_l \exp(-2i\sigma_l)] = \mu \mathrm{d}g(t)/\mathrm{d}t, \tag{3}$$

where μ represents the real part of the nuclear phase shift. The function $g(t)$ is taken to be

$$g(t) = \{1 + \exp[(T-t)/\Delta]\}^{-1} \qquad \text{(Woods-Saxon shape)}, \tag{4}$$

where $t = l + \frac{1}{2}$, T is the interaction radius and Δ the rounding parameter which describes the width of the transition zone. These parameters are expressed in angular momentum units. In semi-classical approximation $T = kR$ and $\Delta = kd$, where R is the interaction radius and d the thickness of the transition zone. Condition (4), when substituted in formulae (2) and (3) describes a gradual transition from complete absorption, for partial waves with impact parameters much smaller than the nuclear radius to pure Coulomb scattering for partial waves outside the nucleus.

For cases in which Coulomb effects may be neglected the Coulomb phase shifts become zero and the cross section for angles where $4T(\pi-\theta) \gg 1$ becomes

$$\frac{d\sigma}{d\Omega} = \frac{T^4}{k^2}[F(\Delta\theta)]^2\left(\frac{\theta}{\sin\theta}\right)\left\{(1-\varepsilon_1)^2\left[\frac{J_1(T\theta)}{T\theta}\right]^2 + \left(\frac{\mu}{T}\right)^2\left[\frac{J_0(T\theta)}{T\theta}\right]^2\right\}. \quad (5)$$

Here ε_1 is a measure of the transparency of the nuclear interior. The form factor $F(\Delta\theta)$ depends on the shape of $g(t)$. For the case of a "Woods-Saxon" shape, $F(\Delta\theta)$ is

$$F(\Delta\theta) = (\pi\Delta\theta)\{\sinh(\pi\Delta\theta)\}^{-1}. \quad (6)$$

TABLE 1

The values of the strong absorption parameters which were used to calculate the fits to the experimental curves as shown in figs. 3 and 4

Element	Blair model	USAM					
	R_{0C} (fm)	R_C (fm)	d (fm)	μ	ε_1	n	Theory
^{9}Be	5.8	5.4	0.25	0.35	0.27	0.2	uncharged
						0.2	charged
^{12}C	5.9	5.4	0.16	0.28	0.29	0.3	uncharged
						0.3	charged
^{16}O	6.6	5.8	0.37	0.54	0.00	0.5	uncharged
		6.1	0.26	0.47		0.5	charged
^{27}Al	6.8	6.7	0.52	0.57	0.00	0.7	uncharged
		6.8	0.53	0.00		0.7	charged
^{32}S	7.4					0.9	uncharged
		7.1	0.44	−0.08		0.9	charged

The interaction radii R_{0C} and R_C are the radii R_0 and R respectively, corrected for Coulomb influence.

In the limiting case, where μ, Δ and ε_1 approach zero, $g(t)$ becomes a unit step-function at $t = T$ which is in effect the Blair sharp cut-off condition and eq. (5) reduces for small angle scattering ($\theta < 10°$) to eq. (1). When USAM is used to explain the scattering of charged particles from the heavier nuclei of the group considered here, Coulomb effects can no longer be neglected and the cross-section expression becomes much more involved. Frahn and Venter [10]) derive a closed expression and formulate a simplified model [11]) for the case where $\varepsilon_1 = 0$, which means that the nucleus is totally absorbing.

The values of the parameters used with the Blair model and USAM for both the charged and uncharged cases are given in table 1. The parameters were obtained with automatic search programmes which minimized the mean-squared deviation between the calculated and experimental cross sections.

The interaction radii R_C given in table 1, were obtained with theories for uncharged particles and were corrected for Coulomb influences by using the relationship [5])

$$R = R_C[1-(2n/kR_C)]^{\frac{1}{2}}, \text{ where } n = mZ_1Z_2e^2/(h^2k).$$

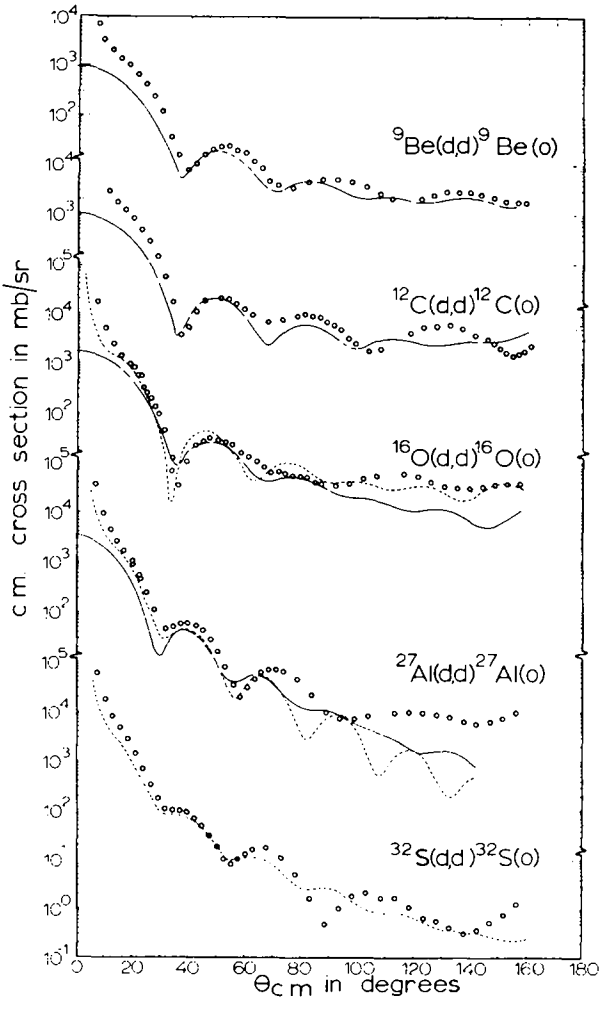

Fig. 4. The cross sections for elastic scattering of deuterons from ^{9}Be, ^{12}C, ^{16}O, ^{27}Al and ^{32}S as a function of scattering angle. The circles are the experimental points, the solid lines the best fits using the uncharged version of USAM and the dashed lines the best fits using the charged version of USAM.

For light nuclei the influence of the Coulomb interaction on the value of d is small and could be neglected.

As can be seen from eqs. (5) and (6), the width Δ of the transition zone determines the average slope of the cross-section curve, while the factor μ controls the filling in

of the minima. With physically acceptable values of the R and d parameters, the phenomenological fits to the experimental data shown in fig. 4 are quite reasonable. Both charged and uncharged versions of USAM are presented in the cases of ^{16}O and ^{27}Al. A good fit for angles between 0° and 90° can be obtained, but then the predicted backward cross sections are in error by factors of 2 to 4. Since the values of the parameters d and μ are more sentitive to the cross section at large angles it was decided to present the best overal fit.

The interaction radii, which are formally the sum of those of the projectile and target nuclei, show the same trend as the Blair model interaction radii (increase with mass number) but are slightly smaller. The lighter elements ^{9}Be, ^{12}C and ^{16}O seem to have a smaller transition zone than the heavier elements ^{27}Al and ^{32}S.

The value of the real phase shift parameter μ differs considerably for the two sets of parameters of ^{27}Al. This is to be expected since a large value of μ partially compensates for the neglected Coulomb effects. For the heavier elements the μ parameters become effectively zero, which is in agreement with the results published by Frahn and Jansen [13]).

In order to obtain better fits to the ^{9}Be and ^{12}C results, it was necessary to use non-zero values of the coefficient ε_1, which is a measure of the transmissive properties of the nuclear interior. This would imply that the ^{9}Be and ^{12}C nuclei are partially transparent to deuterons, which is somewhat unexpected if the low binding energy of the deuteron is considered. On the other hand it may indicate that the deuteron wavelength is comparble to that of the nuclear radius so that the wave could get around the nucleus without being totally absorbed.

5.4. THE OPTICAL MODEL

A modified version of the computer programme SCAT 4 (ref. [12])) was used to obtain the optical model parameters. The parameters were adjusted in order to minimize the mean-squared deviation χ^2 between the calculated and experimental cross sections.

In the analysis the contributions due to spin-orbit interactions were neglected. The optical potentials used were composed of the sum of the following potentials:
real part

$$V(r) = -Vf(r, R_1, a_1),$$

imaginary part

$$W(r) = -4a_2 W|\mathrm{d}f(r, R_2, a_2)/\mathrm{d}r|,$$

Coulomb part

$$V_C(r) = (3-r^2/R_{Coul}^2)Ze^2/(2R_{Coul}) \qquad \text{for } r \leqq R_{Coul},$$
$$V_C(r) = Ze^2/r \qquad \text{for } r > R_{Coul},$$

The function

$$f(r, R, a) = \{1+\exp[(r-R)/a]\}^{-1}$$

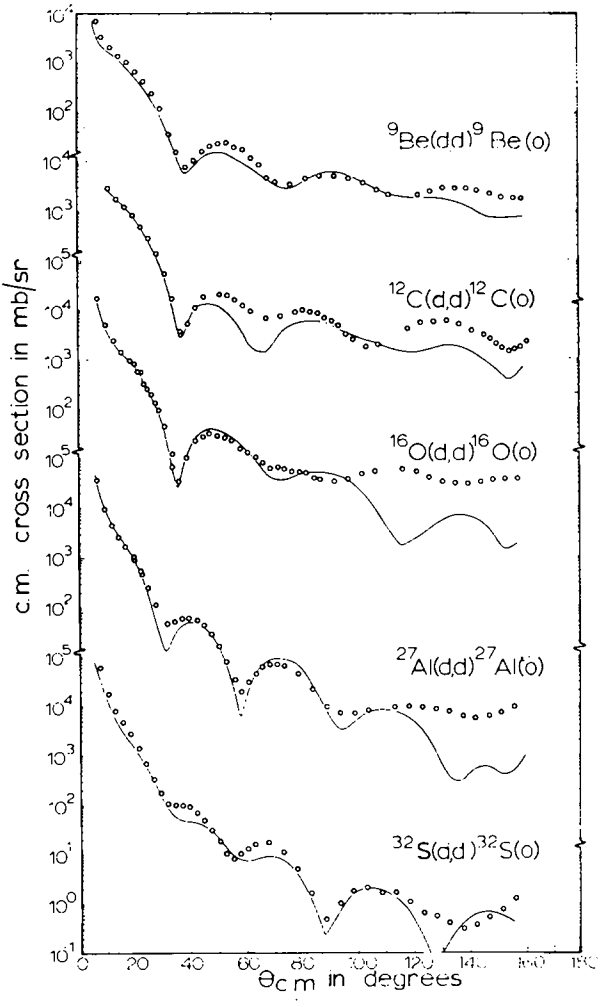

Fig. 5. The cross sections for elastic scattering of deuterons from ^{9}Be, ^{12}C, ^{16}O, ^{27}Al and ^{32}S as a function of scattering angle. The circles are the experimental points and the solid lines are the best fits using the optical model.

TABLE 2

The values of the optical model parameters used for the calculated cross section in fig. 5

Nucleus	V (MeV)	r_1 (fm)	a_1 (fm)	W (MeV)	r_2 (fm)	a_2 (fm)
^{9}Be	65.0	1.250	0.790	7.2	1.250	1.025
^{12}C	63.0	1.250	0.820	8.0	1.250	0.930
^{16}O	100.0	1.250	0.705	15.0	1.225	0.605
^{27}Al	84.0	1.250	0.765	15.5	1.275	0.645
^{32}S	90.0	1.250	0.620	20.0	1.300	0.580

is the Woods-Saxon form factor and $R = r_0 A^{\frac{1}{3}}$. The factor $4a_2$ in the imaginary potential is introduced to normalize the derivative of the form factor to unity at its maximum value. The Coulomb potential is that due to a uniform charge distribution within a sphere of radius R_{Coul}, where $R_{\text{Coul}} = r_{\text{Coul}} A^{\frac{1}{3}}$. The radius parameter r_{Coul} was taken throughout to be 1.3 fm.

The best fits obtained, together with the experimental results are shown in fig. 5. The parameters used to obtain the calculated cross sections are given in table 2.

It is known [14]) that fits of essentially the same quality can be found for any reasonable value of the real radius parameter r_1, therefore it was decided to fix r_1 at a value of 1.25 fm. All the remaining parameters were then adjusted to give a best fit. Having obtained this fit a change in the assumed value of r_1 did not improve the fit. The ambiguity in the depth of the real potential [14]) was resolved by giving preference to fits for which V was in the region of 100 MeV. This value results from the work of Watanabe [15]). In the cases of ^{9}Be and ^{12}C, satisfactory fits could not be found in this region of V, therefore the real potentials which were in the region of 65 MeV were used for these two nuclei. No attempt was made to find best fits for real potentials which were very much deeper than 100 MeV. The fact that both V and W for ^{9}Be and ^{12}C are lower than those for the other nuclei might again be taken as an indication that, in a semi-classical approximation, the deuteron wave length is comparable to the radii of the two light nuclei.

As has been pointed out previously [16]), strong inelastic scattering to the collective states may appreciably affect the elastic scattering in a way which cannot be taken into account by a central complex potential alone. It was found in this experiment that at angles larger than 60° the inelastic scattering cross sections for the first excited states of the even-mass nuclei are comparable with or even larger than the elastic cross sections. The relatively poor fits obtained at larger angles would indicate that the effect of the inelastic scattering on the elastic should be taken into account by a coupled channels calculation.

It is a pleasure to thank the cyclotron staff for their enthusiastic co-operation, G. Burdzik for assistance with measurements and analysis of data, Professor W. E. Frahn for helpful discussions and the staff of the University of the Witwatersrand's IBM 1620 computer for assistance with Blair model and USAM calculations. One of us (M.J.S.) would like to express her appreciation for the hospitality of the CSIR.

Appendix EXPERIMENTAL RESULTS

TABLE A1

Cross sections for the elastic scattering of 15.8 MeV deuterons from ^{9}Be

$\theta_{c.m.}$ (deg)	$\frac{d\sigma(\theta)}{d\Omega}$ c.m. (mb/sr)
6.1	1.35×10^{4}
7.3	6.76×10^{3}
9.2	3.28×10^{3}
12.2	1.95×10^{3}
15.2	1.30×10^{3}
18.3	9.36×10^{2}
21.3	6.18×10^{2}
24.3	3.78×10^{2}
27.3	2.12×10^{2}
30.4	1.03×10^{2}
33.3	3.15×10
36.4	1.29×10
39.3	6.57
42.3	9.15
45.3	1.42×10
48.2	1.80×10
51.2	2.03×10
54.0	2.15×10
56.9	1.73×10
59.8	1.51×10
62.6	9.98
65.5	7.44
68.3	3.95
71.1	3.26
76.6	3.05
82.1	3.94
87.4	4.42
92.6	4.56
97.8	4.09
102.8	3.29
107.8	2.30
111.7	1.90
122.1	1.89
126.6	2.27
131.1	2.60
135.5	2.70
139.8	2.63
144.0	2.30
148.2	1.97
152.3	1.68
156.4	1.63
159.3	1.64

TABLE A2

Cross sections for the elastic scattering of 15.8 MeV deuterons from ^{12}C

$\theta_{c.m.}$ (deg)	$\frac{d\sigma(\theta)}{d\Omega}$ c.m. (mb/sr)
11.5	2.65×10^{3}
14.4	1.63×10^{3}
17.3	1.10×10^{3}
20.1	7.24×10^{2}
23.0	4.31×10^{2}
25.8	2.56×10^{2}
28.7	1.28×10^{2}
31.5	4.68×10
34.3	1.49×10
37.1	3.28
39.9	4.42
42.7	9.55
45.6	1.61×10
51.1	1.88×10
53.8	1.72×10
56.6	1.41×10
59.4	1.09×10
62.1	8.05
67.5	5.92
72.9	6.37
78.2	7.70
80.8	8.23
83.4	7.82
86.0	7.20
88.6	5.82
91.2	5.08
93.7	4.04
96.2	2.83
98.7	2.07
103.7	1.50
107.6	1.65
118.2	3.52
112.9	4.66
127.5	4.80
132.1	5.26
136.6	4.48
141.1	3.39
145.6	2.68
147.8	2.15
150.0	1.70
152.2	1.40
154.3	1.23
156.5	1.31
158.6	1.50
160.8	1.99

TABLE A3

Cross sections for the elastic scattering of 15.8 MeV deuterons from ^{16}O

$\theta_{c.m.}$ (deg)	$\frac{d\sigma(\theta)}{d\Omega}$ c.m. (mb/sr)
4.4	2.91×10^{6}
7.2	1.71×10^{4}
10.0	5.19×10^{3}
12.8	2.49×10^{3}
15.6	1.42×10^{3}
18.4	9.41×10^{2}
20.2	8.50×10^{2}
21.2	5.56×10^{2}
22.5	5.37×10^{2}
24.0	3.22×10^{2}
25.2	2.47×10^{2}
26.5	1.94×10^{2}
26.8	1.56×10^{2}
28.0	1.30×10^{2}
29.3	9.17×10
30.8	4.43×10
33.6	9.30
36.4	3.24
39.1	9.80
41.9	2.11×10
44.6	2.62×10
47.3	3.16×10
50.1	2.96×10
52.8	2.54×10
55.5	2.12×10
58.2	1.64×10
60.9	1.24×10
63.6	1.01×10
66.2	7.87
68.9	6.95
71.5	6.29
74.1	5.79
76.7	5.19
79.3	5.05
81.9	4.85
84.5	3.71
87.1	3.53
92.2	3.17
97.2	3.61
102.2	4.42
107.1	5.17
116.7	5.64
121.5	5.09
126.2	3.98
130.9	3.15
135.5	2.82
140.1	2.81
144.6	3.09
149.1	3.51
153.6	3.69
158.0	3.69

TABLE A4

Cross sections for the elastic scattering of 15.8 MeV deuterons from ^{27}Al

$\theta_{c.m.}$ (deg)	$\frac{d\sigma(\theta)}{d\Omega}$ c.m. (mb/sr)
4.2	3.17×10^{5}
6.9	3.67×10^{4}
9.6	9.85×10^{3}
12.2	4.59×10^{3}
14.6	2.60×10^{3}
14.9	2.56×10^{3}
17.3	1.63×10^{3}
17.6	1.52×10^{3}
19.3	1.14×10^{3}
20.0	1.07×10^{3}
20.3	8.71×10^{2}
21.5	7.07×10^{2}
22.6	5.25×10^{2}
22.9	4.56×10^{2}
24.1	3.85×10^{2}
25.3	2.45×10^{2}
25.6	2.15×10^{2}
26.8	1.45×10^{2}
28.0	1.10×10^{2}
29.5	6.49×10
32.1	4.48×10
34.8	4.97×10
37.4	5.70×10
40.1	5.95×10
42.7	5.26×10
45.4	4.11×10
48.0	2.75×10
50.6	1.54×10
53.3	7.45
55.9	3.22
58.5	1.86
61.1	2.84
63.7	4.25
66.3	5.80
68.8	6.57
71.4	6.72
74.0	6.02
79.1	4.15
84.2	2.03
89.2	9.45×10^{-1}
94.2	6.89×10^{-1}
99.2	6.86×10^{-1}
104.2	7.91×10^{-1}
114.0	9.29×10^{-1}
118.8	9.39×10^{-1}
123.7	9.12×10^{-1}
128.5	8.39×10^{-1}
133.3	7.55×10^{-1}
138.0	6.21×10^{-1}
142.7	5.34×10^{-1}
147.4	6.00×10^{-1}
152.1	7.05×10^{-1}
156.8	9.10×10^{-1}

TABLE A5

Cross sections for the elastic scattering of 15.8 MeV deuterons from ^{32}S

$\theta_{c.m.}$ (deg)	$\frac{d\sigma(\theta)}{d\Omega}$ c.m. (mb/sr)
6.4	1.86×10^{5}
8.0	6.40×10^{4}
10.6	1.89×10^{4}
13.3	8.58×10^{3}
15.9	4.94×10^{3}
18.6	2.93×10^{3}
21.2	1.47×10^{3}
23.9	7.25×10^{2}
26.5	3.36×10^{2}
29.2	1.73×10^{2}
31.8	1.06×10^{2}
34.4	9.60×10
37.0	9.51×10
39.7	8.71×10
42.3	6.87×10
44.9	4.64×10
47.5	2.92×10
50.1	1.74×10
52.8	9.62
55.3	7.80
57.9	9.85
60.5	1.26×10
63.1	1.51×10
68.3	1.64×10
73.4	1.05×10
78.5	4.93
83.5	1.48
88.6	4.61×10^{-1}
93.6	9.78×10^{-1}
98.6	1.74
103.5	2.00
108.5	1.54
113.5	1.56
118.4	1.00
123.3	6.11×10^{-1}
128.1	5.43×10^{-1}
132.9	3.78×10^{-1}
137.8	3.03×10^{-1}
142.5	3.53×10^{-1}
147.3	4.84×10^{-1}
152.0	7.15×10^{-1}
156.8	1.09

TABLE A6

Cross sections for the inelastic scattering of 15.8 MeV deuterons from ^{9}Be, $Q = -2.43$ MeV.

$\theta_{c.m.}$ (deg)	$\frac{d\sigma(\theta)}{d\Omega}$ c.m. (mb/sr)
9.2	1.93
12.2	4.24
15.2	4.53
18.3	5.43
21.3	7.36
24.4	8.56
27.3	9.85
30.5	1.07×10
33.4	1.01×10
36.4	9.63
39.4	8.10
42.4	7.56
45.3	6.59
48.3	5.62
51.1	4.95
54.1	5.08
57.0	5.31
59.9	5.36
62.7	5.65
65.6	5.83
68.3	5.15
71.2	5.45
76.7	5.25
82.1	4.79
87.4	4.05
92.7	3.56
97.8	3.49
102.9	3.28
107.8	3.32
111.8	2.98
122.1	2.82
126.7	2.53

TABLE A7

Cross sections for the inelastic scattering of 15.8 MeV deuterons from ^{12}C, $Q = -4.43$ MeV

$\theta_{c.m.}$ (deg)	$\frac{d\sigma(\theta)}{d\Omega}$ c.m. (mb/sr)
8.0	1.26×10
12.0	1.13×10
15.0	1.20×10
18.0	1.17×10
21.0	1.10×10
23.9	1.08×10
29.9	9.60
35.8	8.54
41.6	7.09
44.6	5.63
47.5	4.45
53.2	3.88
56.1	4.38
58.9	4.30
61.7	5.08
64.5	5.14
70.1	5.21
75.6	5.35
81.0	5.26
83.7	5.18
86.3	4.83
88.9	4.69
91.5	4.56
94.1	4.41
96.6	4.25
99.1	4.09
101.6	3.66
106.6	3.12
110.5	2.91
121.5	2.78
125.5	2.88

TABLE A8

Cross sections for the inelastic scattering of 15.8 MeV deuterons from ^{27}Al, $Q = -2.21$ MeV

$\theta_{c.m.}$ (deg)	$\frac{d\sigma(\theta)}{d\Omega}$ c.m. (mb/sr)
21.6	4.20
24.3	5.35
26.9	3.93
29.6	3.59
32.3	2.76
35.0	2.39
37.6	1.97
40.3	1.46
43.0	1.46
45.6	1.04
48.3	9.16×10^{-1}
50.9	1.05
53.5	7.14×10^{-1}
56.2	8.59×10^{-1}
58.8	7.44×10^{-1}
61.4	8.60×10^{-1}
64.0	6.52×10^{-1}
66.6	6.70×10^{-1}
69.2	6.25×10^{-1}
71.8	6.09×10^{-1}
74.3	6.55×10^{-1}
79.5	6.63×10^{-1}
84.5	6.57×10^{-1}
89.6	6.30×10^{-1}
94.6	4.91×10^{-1}
99.6	4.33×10^{-1}
104.5	3.14×10^{-1}
114.3	2.70×10^{-1}
119.2	2.99×10^{-1}
124.0	3.12×10^{-1}
128.8	3.72×10^{-1}
133.5	3.84×10^{-1}
138.3	4.36×10^{-1}
143.0	3.93×10^{-1}
147.6	3.69×10^{-1}
152.3	4.53×10^{-1}
156.9	5.29×10^{-1}

TABLE A9

Cross sections for the inelastic scattering of 15.8 MeV deuterons from ^{32}S, $Q = -2.24$ MeV

$\theta_{c.m.}$ (deg)	$\frac{d\sigma(\theta)}{d\Omega}$ c.m. (mb/sr)
18.5	5.42
21.1	1.20×10
23.8	1.27×10
26.4	1.28×10
29.0	1.09×10
31.7	7.93
34.3	6.62
36.9	5.05
39.5	3.44
42.1	2.78
44.7	2.37
47.3	2.33
49.9	2.84
52.5	2.97
55.1	2.87
57.7	3.09
60.2	3.19
62.7	2.70
67.9	2.53
73.0	2.06
78.1	1.68
83.1	1.58
88.2	1.22
93.2	7.41×10^{-1}
98.2	7.23×10^{-1}
103.3	7.79×10^{-1}
108.2	6.84×10^{-1}
113.2	8.58×10^{-1}
118.1	8.21×10^{-1}
123.0	8.38×10^{-1}
127.9	5.82×10^{-1}
132.7	5.15×10^{-1}
137.5	3.36×10^{-1}
142.3	4.34×10^{-1}
147.1	5.13×10^{-1}
151.9	4.73×10^{-1}
156.7	5.44×10^{-1}

References

1) J. S. Blair, Phys. Rev. **115** (1959) 928
2) D. K. McDaniels, J. S. Blair, S. W. Chen and G. W. Farwell, Nuclear Physics **17** (1960) 614
3) C. Mayer-Böricke, R. Santo and U. Schmidt-Rohr, Report Jül-30-Kp; (Max-Planck-Institut für Kernphysik, Heidelberg, Germany (1961))

4) J. S. Blair, G. W. Farwell and D. K. McDaniels, Nuclear Physics **17** (1960) 641
5) W. E. Frahn and R. H. Venter, Ann. of Phys. **24** (1963) 243
6) F. A. Aschenbrenner, Phys. Rev. **98** (1955) 657
7) B. Wolfe, A. Silvermann and J. W. de Wire, Rev. Sci. Instr. **26** (1955) 504
8) L. Wåhlin, Nucl. Instr. **14** (1961) 281
9) U. Hauser and W. Kerler, Rev. Sci. Instr. **29** (1958) 380
10) R. H. Venter, Ann. of Phys. **25** (1963) 405
11) R. H. Venter and W. E. Frahn, Ann. of Phys. **27** (1964) 401
12) M. A. Melkanoff, D. S. Saxon, J. S. Nodvik and D. G. Cantor, A Fortran program for elastic scattering analyses with the nuclear optical model (University of California Press, Berkeley, 1962)
13) W. E. Frahn, and L. P. C. Jansen, Nuclear Physics **59** (1964) 641
14) P. E. Hodgson, Comptes Rendus du Congrès International de Physique Nucléaire (Centre National de la Recherche Scientifique, Paris, 1964) sect. 4b, p. 257
15) S. Watanabe, Nuclear Physics **8** (1958) 484
16) B. Buck, Phys. Rev. **130** (1963) 712